Evidence of six-particle Coulomb correlations in six-wave-mixing signals from a semiconductor quantum well

V. M. Axt

Institut für Festkörpertheorie, Westfälische Wilhelms Universität Münster, Wilhelm-Klemm-Strasse 10, D-48149, Münster, Germany

S. R. Bolton,* U. Neukirch,† L. J. Sham,‡ and D. S. Chemla

Department of Physics, University of California and Materials Sciences Division, Lawrence Berkeley National Laboratory,
1 Cyclotron Rd., MS 2-346, Berkeley, California 94720

Six-wave-mixing signals from a ZnSe quantum well are analyzed experimentally and with a microscopic density-matrix description using the dynamics-controlled-truncation scheme. For each physically distinct combination of polarizations of the exciting pulses, the spectrum of six-wave-mixing emission is measured as a function of time delay. The experimental results are compared with calculations performed at different levels of approximation. Although the leading order contributions to six-wave-mixing signals are of fifth order in the laser field, we show that there are significant signal components that are due to at least $\chi^{(7)}$ processes. The sensitivity of six-wave-mixing signals to high-order Coulomb correlations is demonstrated. Six-point density matrices are found to be indispensable for the interpretation of our experiments, while some details seem to indicate the involvement of even higher-order correlation functions. Furthermore, we find a remarkable dynamical decoupling of spectral signatures and the delay-time behavior after excitation with linearly polarized pulses.

I. INTRODUCTION

Predicting the dynamical response of correlated quantum mechanical systems is a long-standing challenge for microscopic theories. Most remarkable is the ability of such systems to be in correlated states, i.e., to form coherent superpositions of states with well-defined relative phases. While in a classical statistical ensemble only incoherent superpositions of the ensemble members are possible, in a quantum system, superpositions of the phase-sensitive probability amplitudes can be realized. The result is a high degree of entanglement, which could not be reached within a classical ensemble. The rich phenomenology associated with this fundamental difference between quantum and classical systems is most clearly illustrated in atomic physics.[1] Dense many-body systems, such as semiconductors, also support strong Coulomb correlations. The effects of these correlations are, however, very hard to access because of their complexity. Despite conceptual and practical difficulties, significant theoretical progress was made recently in the description of Coulomb correlations in condensed matter.[2–16] Much attention has been devoted to systems with strongly correlated dynamics for which it is not justified to treat the interaction between quasiparticles as scattering events local in space and time, a key assumption of the Boltzmann theory. With the development of advanced spectroscopy techniques whose time resolution is much shorter than the scattering time scales, such effects have become observable. These advances have triggered both experimental and theoretical investigations of electron-electron interaction[17–30] and electron-phonon interaction.[31–39] The two most frequently used nonlinear optical techniques are four-wave-mixing (FWM) and pump and probe spectroscopy (PP). Modeling the associated memory effects requires a quantum kinetic description be-

yond the Boltzmann limit.[21–23,27–29] The issues that have been addressed at the quantum kinetic level cover a wide range of phenomena, including the dynamics of screening,[4,21,22] the dynamics of dephasing,[23] the signatures of the energy-time uncertainty,[17,18,34,35] phonon-quantum beats,[31,38,39] biexcitonic correlations,[9,40] and the effects of exciton-exciton continuum correlations.[24–26,41,42] The successful theoretical description of these phenomena depended crucially on the ability to find a reduced description of the dynamics in which the relevant correlations are built up from correlations involving only a limited number of quasiparticles, e.g., only a few electron-hole pairs.

The simplest such theory accounts explicitly for only two-particle correlations, and yields the semiconductor Bloch equations.[43,44] It is able to reproduce a fairly wide variety of phenomena. Recent comparative experimental and theoretical studies of FWM signals performed in semiconductors show features related to genuine four-particle correlations.[24–28] Such experiments are usually carried out at low intensities to avoid correlations involving more than four particles. At high intensities, they cannot discriminate such correlations. Thus, so far, experiments have not tested effects of higher-order correlations, and consequently, only very few theoretical studies have at all considered correlations at the six-particle level.[40,45,46] In Ref. 40, a system close to the coherent regime has been studied and the effect of six-particle correlations turned out to be restricted to an almost negligible excited state absorption in this case. Meier and Koch[45] analyzed the opposite limit, namely, a situation where all carriers are assumed to be completely incoherent and present in the system from the start. On the basis of a simplified one-dimensional tight-binding model with ten lattice sites, they predict the following features of differential transmission changes related to six-particle correlations: (a) a

noticeable excited state absorption, (b) an enhancement of the bleaching compared with the result obtained from Pauli-blocking, and (c) a strong compensation of single-pair transitions directly induced from the incoherent thermalized excitons. Similar compensation effects have been observed in the phase of a FWM signal.[46] Strong compensations, however, make it hard to separate effects related to six-particle correlations from other influences and to highlight their dynamical properties directly. While it is easy to suppress nonlinearities from two-particle contributions and make four-particle correlations the leading nonlinear contribution, e.g., in PP using counter-circularly polarized beams, there is no such possibility on the six-particle level. And indeed, it was observed that in PP experiments with counter-circularly polarized pulses the signal is dominated by four-particle correlations.[40,47,48] Two-beam FWM is less selective since two-particle correlations cannot be totally suppressed to leading order in this case. Therefore, it is natural to ask under which circumstances correlations involving more than four particles may play a more prominent role. Although in six-wave-mixing (SWM) experiments the two- and four-particle correlations cannot be suppressed via polarization selection rules, one may expect a larger relative weight of the six-particle contribution than in FWM or PP.[49]

In the present paper we demonstrate that, in contrast to FWM, SWM emission shows clear signatures of high-order correlations involving at least six-particles. While a previous investigation[50] concentrated on a single combination of polarization vectors, we analyze here all relevant polarization configurations and also provide for a detailed derivation of the theory used in the present paper, as well as in Ref. 50.

In order to enable a meaningful comparison between theory and experiment, it is important to deal with a well-characterized system. In the present paper, we study a $ZnMg_xSSe_{x-1}/ZnSe/ZnMg_xSSe_{x-1}$ single quantum well; a system that is ideally suited for studies of correlated many-body quantum kinetics. Our investigation benefits particularly from several properties of this structure. First, the binding energies for the exciton and biexciton, as well as the heavy-hole–light-hole splitting are fairly large and the corresponding linewidths are narrow. This allows for the selective excitation of heavy-hole excitons and biexcitons, and gives a clearly resolved spectral response. In addition, the strong optical nonlinearities allow a single, 5 nm quantum well to generate easily measurable experimental signals. Thus we avoid corruption of the signal by propagation effects. These two advantages provide an extremely clean experimental system that greatly facilitates interpretation and quantitative comparison with theory.

Previous work on this experimental system, such as the analysis of the transient polarization state of FWM emission,[27,28] has demonstrated the presence of rather complicated dynamical features that have been identified as signatures of four-point Coulomb correlations. It is important to note that in the case of undoped direct-gap semiconductors, these correlations are dynamically generated. Even though the ground state of the semiconductor has correlations, these do not play a role in the consideration of the excited electrons and holes near the direct gap. These electrons and holes

behave as particles with mutual interactions without affecting the ground state that, except for providing the dielectric screening, can be considered as rigid.[51] We thus have a well-defined starting point for the dynamics that is completely uncorrelated. The strong correlations due to the Coulomb interaction build up in the system only after the carriers are excited. The absence of correlations before the excitation is a great advantage for our purposes, because it greatly facilitates the calculations of the ultrafast optical response compared to systems with strong ground-state correlations, and thus allows for much more conclusive comparisons with measurements. Furthermore, as the correlations are induced by the laser field, they show a strong dependence on the excitation conditions. This allows for partial external control over the correlations and their dynamical properties. In strongly correlated materials, the excited particles experience extremely large couplings among themselves and with other low-lying excitations and, therefore, we believe that optical investigations similar to ours will shed light on the effects of electronic correlation in these systems.

In this paper we will show that it is indeed possible to find excitation and detection conditions where high-order Coulomb correlations have a significant qualitative impact on optical signals from semiconductor quantum wells. In particular, we will discuss the influence of the correlated part of the six-point density matrix describing transitions from incoherent exciton densities to correlated two-pair states. It turns out that SWM signals provide a sensitive monitor for this type of a quantum-kinetic correlation. We compare our experimental results quantitatively with the results of a microscopic density-matrix theory using the dynamics-controlled-truncation (DCT) scheme.[10,11] Comparisons are made with theory at three different levels of sophistication: (a) a fully coherent description following only the dynamics of coherent single-pair and two-pair transition amplitudes, (b) a treatment that, in addition, accounts for incoherent densities, and (c) a level of description that includes, in addition to the terms in (a) and (b), correlated six-point density matrices representing transitions from incoherent excitons to bound or unbound two-pair states. Our results clearly indicate that the contribution from these six-point correlations is crucial to a correct description of the optical response of this system.

II. EXPERIMENTAL SETUP

Spectrally resolved, degenerate SWM experiments were performed on a 5 nm $ZnMg_xSSe_{x-1}/ZnSe/ZnMg_xSSe_{x-1}$ single quantum well. In this sample, the hh-lh splitting is $E_{lh-hh} = 20$ meV and the binding energies for the exciton X and the biexciton X_2 are $E_X^b = 25$ meV and $E_{X_2}^b = 6.6$ meV. The hh-X and hh-X_2 transitions can therefore selectively be excited, yielding a well-resolved spectral response (see linear absorption in Fig. 1)

The sample was held in a liquid He cryostat at $T = 10$ K, giving a hh-X peak centered at $\hbar\Omega_X = 2.825$ eV. 70 fs transform limited pulses from a frequency doubled Ti:Sapphire laser were used for excitation, and were tuned to excite exclusively the $1s$ hh-X. The excitation density was approximately $N = 10^{10}$ cm^{-2}. As detailed below, low-excitation
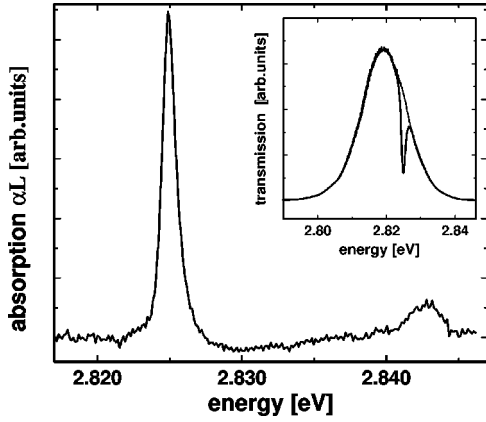
FIG. 1. Linear absorption of the sample. Inset: transmission (thick line), laser spectrum (thin line).

FIG. 2. Measured six-wave-mixing emission shown over three orders of magnitude in emission intensity. (a) in the $\{x,y,y\}$ configuration, (b) in the $\{x,x,x\}$ configuration.

densities are favorable for our purposes. Therefore, we kept the intensity as low as possible. However, SWM signals involve rather high powers in the laser field and thus fall off quite rapidly, while the noise (much of which comes from scattered light) scales linear with the intensity. The resulting loss of the signal to noise ratio severely limits the accessible intensity range. Varying the intensity within these limits we found that (a) the results presented below are rather insensitive to these intensity changes and (b) even for the lowest accessible intensities, the regime of a strict power-law scaling of the SWM signal is not reached. Two laser pulses with wave vectors $\vec{k}_1$ (pulse 1) and $\vec{k}_2$ (pulse 2) separated by the time delay Δt excite the sample, and the SWM signal is measured in the momentum conserving direction $\vec{k}_s = 3\vec{k}_2 - 2\vec{k}_1$. Our convention is that $\Delta t > 0$ if pulse 1 precedes pulse 2. The polarizations $\sigma_{1,2}$ of the exciting pulses were varied among all significant combinations of circular and linear, and the SWM emission was projected onto each of the $\sigma_s = x, y, \sigma^+$, and σ^- polarizations. The spectrum of each σ_s was recorded as a function of Δt. To label the various polarization configurations we use the notation $\{\sigma_1, \sigma_2, \sigma_s\}$.

III. MEASURED SIX-WAVE-MIXING SIGNALS

In this section we present our experimental results. First, we discuss excitation conditions involving linearly polarized pulses, then we address some additional issues related to the more selective excitation created by circular polarizations. For each polarization configuration, the data (experimental in this section and theoretical in the next one) is presented as contour maps, $S_{SWM}(\Delta t, \omega)$, giving the magnitude of the SWM signal on a logarithmic scale as a function of time delay and frequency. The gray scaling corresponds to three orders of magnitude in the intensity starting from the respective maxima. It is important to note that these plots give information both on the time-delay dependence [variation of $S_{SWM}(\Delta t, \omega)$ with Δt] and the real-time dependence [related to the Fourier transform of the variation of $S_{SWM}(\Delta t, \omega)$ with ω]. As shown below, this point is very important for discussing the interpretation of the experiments and the comparison with theory.
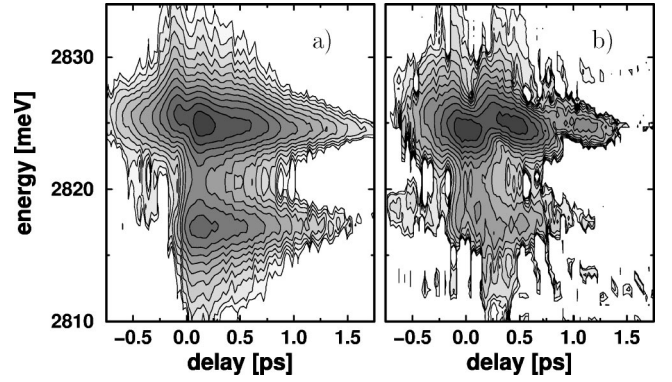
Figure 2(a) displays $S_{SWM}(\Delta t, \omega)$ measured in the $\{x,y,y\}$ configuration. We observe strong contributions around the spectral energy of the exciton $(\hbar\Omega_X)$ and about one biexciton binding energy below $[\hbar(\Omega_{X_2} - \Omega_X) = 2.8184$ eV]. In the remainder of the text we will call this energy the exciton-biexciton-transition (EBT) energy. The X emission peaks at $\Delta t = 150$ fs, and is clearly visible for -750 fs $\leqslant \Delta t \leqslant 2$ ps. It is centered at $\hbar\Omega_X$ for $\Delta t > 0$, but experiences a ≈ 1 meV shift for $\Delta t \approx -200$ fs$\rightarrow 0$. The emission at the EBT energy is visible for -200 fs$\leqslant \Delta t \leqslant +1.5$ ps and is centered at $\hbar\omega = 2.818$ eV for all Δt. It results from two-photon transitions to the biexciton, as well as from transitions between incoherent excitons and two-pair states. Although, overall, the signal has its maximum at the exciton, the biexciton component is strong. Note that neither the signal around the exciton nor that around the EBT energy show any beats, instead in both cases $S_{SWM}(\Delta t, \omega)$ exhibits a smooth decay with increasing Δt. Obviously, the spectral content of the SWM signal showing that considerable transitions to biexcitons have been generated, does not translate into corresponding features in the time-delay dependence. This dynamical decoupling between the real-time dependence, corresponding to the spectral content, and the time-delay dependence is in contrast to predictions made on the basis of simple models that neglect correlations. Indeed, in the general case, and especially when correlations are important, there is *no* fundamental energy-time uncertainty between the ω and Δt dependence of a nonlinear optical signal. In that respect, our observation is in line with previous observations by Siegner *et al.*,[52,53] Wehner *et al.*,[54] and Steinbach *et al.*,[38] where it was found that for the short pulse excitation of correlated systems the t or ω dependence and the Δt dependence of FWM signals contain *different* information.

Figure 2(b) presents $S_{SWM}(\Delta t, \omega)$ measured in the $\{x,x,x\}$ configuration. In this case, the X emission is only visible for -500 fs$\leqslant \Delta t \leqslant 1.4$ ps, but shows clearly at least three beats with maxima at $\Delta t \approx 0$ fs, 500 fs and 1.1 ps, respectively. Here, the maxima are centered at $\hbar\Omega_X \approx 2.825$ eV for all time delays, but the second and third beats are noticeably slanted. As in the $\{x,y,y\}$ case, we also observe an emission at the EBT energy. It is, however, much weaker
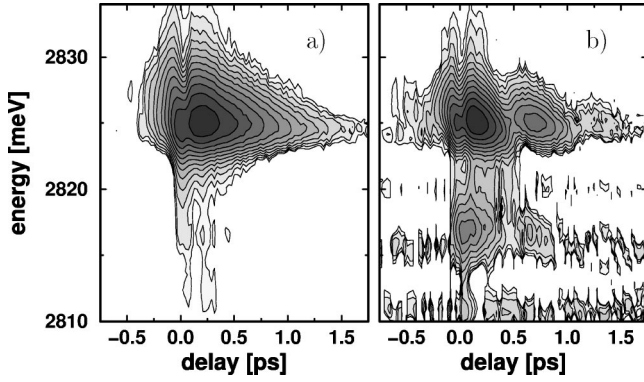
FIG. 3. Measured six-wave-mixing emission. (a) in the $\{\sigma^+, \sigma^+, \sigma^+\}$ configuration, (b) in the $\{x, \sigma^+, \sigma^+\}$ configuration.

than for the $\{x, y, y\}$ configuration, but nevertheless, well distinguishable for -100 fs $\leq \Delta t \leq +500$ fs. Here, the situation is almost reversed compared with the $\{x, y, y\}$ configuration. Now, biexcitonic features are much stronger in the time-delay domain (strong beating) than in the frequency domain (weak EBT line).

Configurations involving circular polarized pulses allow for a more selective excitation, as biexcitonic features can be either totally or partially suppressed. A total suppression of transitions involving the bound biexciton state is possible using cocircular σ^+ pulses for the excitation. The resulting SWM signal is also σ^+ polarized and plotted in Fig. 3(a). As expected, it is emitted exclusively at the spectral position of the exciton and does not exhibit any beats. It is interesting to compare this result with the SWM emission for the $\{x, \sigma^+, \sigma^+\}$ configuration in Fig. 3(b). Selection rules based on angular momentum conservation predict that these two signals should coincide at the $\chi^{(5)}$ level. Obviously, in contrast to the $\{\sigma^+, \sigma^+, \sigma^+\}$ case, the $\{x, \sigma^+, \sigma^+\}$ signal shows biexciton beats forbidden in fifth order. We therefore conclude that this feature has to be attributed to processes that are at least of the seventh order in the field, i.e., $\chi^{(n \geq 7)}$. This high-order contribution persists down to the lowest measurable excitation densities, raising questions about the validity of the perturbation expansion in nonlinear processes with multiple resonances in materials with a strong correlation.[49,55]

IV. THEORETICAL FRAMEWORK

Traditionally, the many-body problem in semiconductors has been approached using the random-phase approximation, in which many-particle correlations are accounted for only on a mean-field level by factorizing high-order correlations in products of elements of the two-point density matrices. This level of theory, which results in the well-known semiconductor-Bloch equations, works adequately for many experimental conditions. For many years it has been state-of-the-art to extend the semiconductor-Bloch equations by using scattering terms derived from the second-order Born approximation leading to equations of Boltzmann-type.[44] However, with decreasing density and on time scales short compared to the mean free quasiparticle scattering time, not

enough scattering events take place for the interactions of quasiparticles to be lumped into a mean field. Instead, the effects of nearby quasiparticles can be resolved individually, thus establishing strong correlations among the carriers.[25] For example, it is well known that in the low-density regime, it is important to account for both *out-scattering* as well as *in-scattering* terms, where the latter are also known as *vertex corrections*.[56-58] At low densities, neglecting vertex corrections would strongly overestimate scattering events with small momentum transfer, i.e., scattering between far away particles,[56,57] while out-scattering terms usually dominate at high densities, where the individual contributions of nearby particles embodied in the vertex corrections are no longer resolved. Furthermore, it is clear that neither mean-field nor Boltzmann-type approaches can account for situations where two-pair correlations, such as biexcitons, play a prominent role. For such experiments it is necessary to include four-point correlations and to treat the Coulomb interaction *nonperturbatively*. The importance of four-particle correlations in the nonlinear optical response of semiconductor heterostructures has been demonstrated in several recent experiments.[24-28,47,48]

An enormous amount of work is currently focused on developing techniques to deal with the dynamics of correlated many-body systems.[2-16] An approach that has proven particularly useful for the description of correlation effects seen in FWM and PP experiments[24-29,40,45,59] is the dynamics-controlled-truncation (DCT) scheme.[10,11] In the DCT scheme, a classification of the higher-order density matrices, according to their respective leading orders in the laser field, is used as controllable truncation criterion. At low densities, where correlation effects are most pronounced, FWM and PP experiments are dominated by contributions of third order in the laser field. FWM and PP experiments, therefore, probe mostly the dynamics of two-point or four-point density matrices. This class of experiments is usually influenced only weakly by six-point and higher-order correlations. In contrast, SWM signals are at least of fifth order in the laser field, where a stronger impact of correlations beyond the four-point level is expected, as indicated by early work on large gap semiconductors.[49,55]

In the present paper, we apply the third-order DCT scheme to truncate the hierarchy of density matrices and select the relevant dynamical variables.[10,11] We account for the dynamics of four types of density matrices defined in Refs. 11 and 40, Y, $\bar{B}$, $\bar{N}$, and $\bar{Z}$. The bar over the symbols $\bar{B}$, $\bar{N}$, and $\bar{Z}$ indicates that the respective uncorrelated parts have been subtracted, so that these variables account for correlated processes beyond the mean-field limit. Table I summarizes the corresponding definitions in the Wannier representation. The dynamical variables fall into two categories, coherent amplitudes and variables accounting for incoherent parts of the dynamics. Y and $\bar{B}$ belong to the first category and represent, respectively, single-pair transitions and the correlated part of two-pair transition amplitudes, i.e., two-photon coherences. These are rapidly oscillating phase-sensitive quantities. Note that $\bar{B}$ contains contributions from both the bound biexcitonic states X_2 and the unbound two-exciton con-

TABLE I. Definition of dynamical variables in terms of expectation values of Fermi operators $\hat{c}_j$ ($\hat{d}_j$) for the annihilation of an electron (hole) in the Wannier state at site j in the conduction (valence) band σ_{c_j} (σ_{v_j}).

$$Y_2^1 \equiv \langle \hat{Y}_2^1 \rangle \equiv \langle \hat{d}_1 \hat{c}_2 \rangle$$

$$\bar{B}_{24}^{13} \equiv \langle \hat{Y}_2^1 \hat{Y}_4^3 \rangle - Y_2^1 Y_4^3 + Y_4^1 Y_2^3$$

$$\bar{N}_{14}^{23} \equiv \langle \hat{Y}_1^{2\,\dagger} \hat{Y}_4^3 \rangle - Y_1^{2*} Y_4^3$$

$$\bar{Z}_{146}^{235} \equiv \langle \hat{Y}_1^{2\,\dagger} \hat{Y}_4^3 \hat{Y}_6^5 \rangle - Y_1^{2*}(\bar{B}_{46}^{35} + Y_4^3 Y_6^5 - Y_6^3 Y_4^5)$$
$$\qquad - \bar{N}_{14}^{23} Y_6^5 - \bar{N}_{16}^{25} Y_4^3 + \bar{N}_{14}^{25} Y_6^3 + \bar{N}_{16}^{23} Y_4^5$$

tinuum X-X. We call the limiting case, where only the coherent transition amplitudes Y and $\bar{B}$ are taken into account the coherent limit (CL). The incoherent parts of the dynamics are represented in our treatment by the density matrices $\bar{N}$ and $\bar{Z}$. $\bar{N}$ describes two physically different aspects of the dynamics: (i) coherences between different pair states related to intersubband and intraband transitions and, (ii) incoherent occupations of pair states. Writing the definition of $\bar{N}$ in the form $\bar{N} = \langle (\hat{Y} - \langle \hat{Y} \rangle)^\dagger (\hat{Y} - \langle \hat{Y} \rangle) \rangle$ suggests an interpretation as the fluctuation of the one-pair amplitude Y. In the following, we refer to a level of theory that in addition to the CL parts accounts for the $\bar{N}$ contributions as the incoherent density (ID) level. Finally, the six-point density matrix $\bar{Z}$ accounts for transitions from incoherent exciton densities to two-pair states. $\bar{Z}$ belongs to the incoherent part of the dynamics, because it can only have finite values in the presence of incoherent densities. Nevertheless, being a transition density, $\bar{Z}$ also has some properties of coherent variables, e.g., it oscillates at optical frequencies and is therefore phase sensitive. In atomic physics it is well known that corresponding contributions lead to phenomena such as *excited state absorption*. Also, the occurrence of new *dephasing induced resonances* is related to transitions of this type.[60,61] We refer to the level of theory that in addition to the CL and ID parts accounts for the transitions described by $\bar{Z}$ as the incoherent-density-assisted transitions (IDAT) level.

As detailed below, we numerically solve the equations of motion of Y and $\bar{B}$ for the CL level, of Y, $\bar{B}$, and $\bar{N}$ for the ID level and of Y, $\bar{B}$, $\bar{N}$, and $\bar{Z}$ for the IDAT level as sets of coupled nonlinear equations. Consequently, our results contain contributions of arbitrarily high orders in the laser field, which would not be obtained by applying strict perturbation theory. It should be noted that in principle, the SWM signal could also be influenced in the leading order in the laser field [i.e., $\mathcal{O}(E^5)$] by other high-order correlation functions such as the correlated part of coherent three-pair transition amplitudes or incoherent two-pair occupation densities. At the present time, a microscopic treatment including all of these contributions is out of reach. However, as shown below, a description based on Y, $\bar{B}$, $\bar{N}$, and $\bar{Z}$ already gives good overall agreement with our experimental findings. We conclude from this that we have identified the contributions

dominating the SWM-signal components tested in our measurements. It is very likely, however, that some fine features of our experimental data call for even more advanced modeling for their explanation.

The SWM signal is calculated from the equation of motion for the single-pair amplitude Y, which determines directly the polarization of the sample.[10,11] In the exciton representation this equation has the form,

$$\hbar[-i\partial_t + \omega_\alpha] y_\alpha = \sum_p \mathcal{M}_\alpha^p E_{\text{opt}}^p + \mathcal{Q}_{\text{nonlinear}}^\alpha. \quad (1)$$

Here, $\mathcal{M}_\alpha^p$ are the components of the dipole matrix elements in direction of the polarization vectors of the two exciting pulses p with field amplitudes E_{opt}^p, and $\hbar\omega_\alpha$ is the energy of an optical transition to the exciton state α. It is useful to decompose the nonlinear source $\mathcal{Q}_{\text{nonlinear}}^\alpha$ into three parts

$$\mathcal{Q}_{\text{nonlinear}}^\alpha = \mathcal{Q}_{\text{CL}}^\alpha + \mathcal{Q}_{\text{ID}}^\alpha + \mathcal{Q}_{\text{IDAT}}^\alpha. \quad (2)$$

$\mathcal{Q}_{\text{CL}}^\alpha$ is the source present in the coherent limit. It can be further subdivided into a coherent mean-field contribution (CMF) and a part representing correlated two-pair transitions (TPT) $\mathcal{Q}_{\text{CL}}^\alpha = \mathcal{Q}_{\text{CMF}}^\alpha + \mathcal{Q}_{\text{TPT}}^\alpha$. The CMF part comprises the Pauli blocking and coherent mean-field Coulomb nonlinearities known from the semiconductor Bloch equations. Written explicitly, these terms read

$$\mathcal{Q}_{\text{CMF}}^\alpha = -\sum_{p\bar{\alpha}\bar{\alpha}'} \mathcal{B}_{\alpha\ \bar{\alpha}}^{\bar{\alpha}'\,p} y_{\bar{\alpha}}^* y_{\bar{\alpha}'} E_{\text{opt}}^p$$
$$+ \sum_{\bar{\alpha}\bar{\alpha}'\bar{\alpha}''} (\mathcal{V}_{H\alpha\ \alpha}^{\bar{\alpha}'\ \bar{\alpha}''} - \mathcal{V}_{F\alpha\ \alpha}^{\bar{\alpha}'\ \bar{\alpha}''}) y_{\bar{\alpha}}^* y_{\bar{\alpha}'} y_{\bar{\alpha}''}, \quad (3)$$

where $\mathcal{B}$, $\mathcal{V}_H$, and $\mathcal{V}_F$ are the blocking, Hartree, and Fock matrix elements, respectively, in the exciton basis. In order to account for correlated two-pair transitions, we used the memory kernel representation derived in[27,41,42]

$$\mathcal{Q}_{\text{TPT}}^\alpha = \int_{-\infty}^t dt' \sum_{\alpha'\bar{\alpha}\bar{\alpha}'} y_{\bar{\alpha}}^*(t) \mathcal{K}_{\alpha\ \alpha}^{\alpha'\ \bar{\alpha}'}(t-t') y_{\alpha'}(t') y_{\bar{\alpha}'}(t'). \quad (4)$$

The memory structure induced by the kernel $\mathcal{K}(t)$ distinguishes our quantum-kinetic treatment of the Coulomb interaction from approaches that approximate the scattering processes as events without duration, as is done in the Boltzmann theory. In particular, the occurrence of spectrally narrow structures such as the biexciton render any treatment local in time invalid. In our numerical analysis we have separated the influences of the bound biexciton, i.e., excitonic molecule X_2, from that of the exciton-exciton scattering continuum X-X by extracting the biexciton contribution from the kernel using a Lorentzian fit to the X_2 line in the Fourier transform of $\mathcal{K}(t)$. As shown below, this procedure allows us to switch off selectively either the continuum or the molecule part in order to evaluate their respective influences on the SWM emission.

We distinguish between two physically distinct contributions to the incoherent parts of the dynamics (a) parts di-

rectly proportional to $Y\bar{N}$ or $E\bar{N}$ and (b) six-point correlations proportional to $\bar{Z}$. The former, labeled ID, are directly generated from incoherent densities. They have been discussed previously[27] and are given by

$$\mathcal{Q}_{\mathrm{ID}}^{\alpha} = -\sum_{p\bar{\alpha}\alpha'} \mathcal{B}_{\alpha}^{\bar{\alpha}' \ p} \bar{n}_{\bar{\alpha}\bar{\alpha}'} E_{\mathrm{opt}}^{p}$$
$$+ \sum_{\bar{\alpha}\bar{\alpha}'\bar{\alpha}''} (\mathcal{V}_{H\alpha}^{\bar{\alpha}' \ \bar{\alpha}''} - \mathcal{V}_{F\alpha}^{\bar{\alpha}' \ \bar{\alpha}''})(y_{\bar{\alpha}'} \bar{n}_{\bar{\alpha}\bar{\alpha}''} + y_{\bar{\alpha}''} \bar{n}_{\bar{\alpha}\bar{\alpha}'}).$$
$$(5)$$

The equation of motion for the incoherent density in the exciton representation $\bar{n}_{\alpha\alpha'}$ is derived in the appendix. A comparison of the structure of the direct incoherent contributions in Eq. (5) with the CL sources in Eq. (3) shows that $\mathcal{Q}_{\mathrm{ID}}^{\alpha}$ can be thought of as the incoherent counterpart of the coherent blocking and mean-field Coulomb nonlinearities. However, a closer inspection of these terms reveals that only half of the ID contributions to the Coulomb nonlinearity are needed to reproduce the corresponding mean-field result;[11] the rest is already a correlation effect, although it has a structure that resembles the mean-field parts. Finally, we incorporate the IDAT contribution in our theory. It is, of course, a numerically nontrivial task to deal with a six-point density matrix in a two-dimensional quantum-well system. In order to account for these parts of the dynamics on the same level as the other contributions, we derive in the Appendix a memory kernel representation that is analogous to our treatment of the two-pair transitions. The resulting contribution to the equation of motion for the single-pair transitions is given by

$$\mathcal{Q}_{\mathrm{IDAT}}^{\alpha} = \int_{-\infty}^{t} dt' \sum_{\alpha' \bar{\alpha}\bar{\alpha}'} \mathcal{K}_{\alpha}^{\alpha' \ \bar{\alpha}'}(t - t') e^{i\omega_{\bar{\alpha}}^{-}(t-t')}$$
$$\times [\bar{n}_{\bar{\alpha}\alpha'}(t') y_{\bar{\alpha}'}(t') + \bar{n}_{\bar{\alpha}\bar{\alpha}'}(t') y_{\alpha'}(t')]. \quad (6)$$

It should be noted that the memory kernel representation used here is fully equivalent to the original DCT equations derived in Ref. 10. Another important point is that the kernel $\mathcal{K}(t)$ appearing in Eq. (6) is identical to the kernel $\mathcal{K}(t)$ of Eq. (4) that is needed for the two-pair transitions [cf. also the derivation in the Appendix]. Comparing Eqs. (3) and (4) with Eqs. (5) and (6), it is striking that the coherent mean-field part and the two-pair transitions are related to each other in almost the same way as the ID contribution is related to $\mathcal{Q}_{\mathrm{IDAT}}$. In that respect, it is worth summarizing what was learned from previous investigations of FWM experiments on samples similar to ours. It was pointed out in Res. 29,41, and 62 that in FWM there are strong cancellations between coherent mean-field contributions and the correlated part of the two-pair scattering continuum. Thus, it is natural to expect these interferences to have an incoherent counterpart in the competition between the ID and IDAT contributions. In fact, such a tendency has been reported in Ref. 45 in an analysis of the influence of thermalized exciton densities on PP experiments. The situation is, however, a bit more subtle in the case of FWM experiments. On one hand, the fact that

CL calculations under many circumstances give qualitatively good agreement with experiments may be taken as an indication of cancellations of incoherent contributions. For example, in Refs. 62 and 63 the ratio between the FWM signal at the exciton and the biexciton energies was well reproduced for all pulse polarizations. On the other hand, the coherent limit fails to describe correctly transient polarization states in the FWM, while calculations that in addition, account for $\mathcal{Q}_{\mathrm{ID}}^{\alpha}$, give very good results.[27,28] In fact, a numerical solution at the ID level gives excellent agreement with the FWM experiments even at densities for which $\chi^{(5)}$ contributions are already noticeable[27,28] and adding the IDAT contribution does not significantly change these results[46]. Clearly, the transient polarization of the FWM signals shows no significant compensation between ID and IDAT contributions, whereas the phases of the same signals do exhibit a strong compensation of incoherent parts.[46] We can thus conclude that, although the effects of $\bar{Z}$ are not the same for all aspects of FWM signals, they are either not significant, or are limited to a compensation with other (ID) contributions. This confirms that the FWM is largely insensitive to six-point correlations.

In our calculations we have included all states on the $1s$ heavy-hole parabola and accounted for the twofold degeneracy of the conduction and heavy-hole bands. The exciton eigenfunctions have been calculated by direct diagonalization of the exciton Hamiltonian for a quantum well in k space representation. The Hamiltonian has been discretized with 600 k points with a cutoff at 17 inverse bulk Bohr radii and the following material parameters were taken: electron mass $= 0.14\ m_0$, hole mass$=0.67\ m_0$ [$m_0=$ free electron mass], static dielectric constant$=8.7$. The intregrals defining the blocking, Hartree- and Fock-matrix elements have been performed making use of adaptive step-size Gauss-Romberg routines with automatic error control. In order to determine the memory kernel we followed, Ref. 41, where it was shown that $\mathcal{K}$ can be obtained from an integral equation that can be solved separately from the dynamics. After discretization, the solution has been obtained by standard routines for matrix inversion. In the discretization of the integral equation we did an importance sampling in order to account for the resonance structure of the integrand. Plots of memory kernel components in the frequency regime calculated in this way for a two-dimensional system have been shown in Ref. 27. Also, the quality of the extraction of the molecular part from the two-pair continuum is demonstrated there. As discussed in Ref. 27 we find a broad continuum that does not exhibit any sharp resonance structures that may be identified with antibound states that are sometimes introduced *ad hoc* in the literature. Finally, the dynamic equations have been integrated in time by a standard fourth-order Runge-Kutta routine with a constant time step of 2 fs. Adaptive time-step routines have also been tested. However, it turned out that they gave identical results but with considerably increased computation time. All subroutines have been tested separately and it was verified that a further increase in the number of calculated points or using an increased precision in some of the subroutines has no influence on the final results. Following Refs. 64 and 65, we have accounted for the wave

vectors of the light pulses only parametrically by invoking a discrete Fourier decomposition of our dynamical variables. As shown in Refs. 64 and 65, the transition density Y has nonzero Fourier components for wave vectors of the form $\vec{k} = (\vec{k}_1 + \vec{k}_2)/2 + j \times (\vec{k}_1 - \vec{k}_2)/2$, where j may be any positive or negative odd number. We have kept all nonzero Fourier components in the range $-7 \leq j \leq 7$ and in the corresponding decompositions of $\bar{B}$, $\bar{N}$, and $\bar{Z}$ all Fourier components that can be generated from sources involving the above parts of Y have been accounted for. Note, that the SWM signal corresponds to $j = -5$. It turns out that further restricting the Fourier decomposition to the range $-5 \leq j \leq 5$ has no significant impact on our results. We therefore conclude that the Fourier expansion is rapidly converging and that higher-order Fourier components couple back to the lower orders only very weakly for our excitation conditions. A typical run solving for the dynamics finishes within 2–3 days on a DEC alpha workstation. For the interband dipole matrix elements we have used the standard selection rules that follow from the momentum representation of the states at the center of the Brillouin zone. All equations have been supplemented by dephasing constants. Recently, it was found experimentally that at low temperatures, the dephasing of one-pair and two-pair transitions are of the same order of magnitude.[66] Therefore, for simplicity we have set the damping constants of all transition variables equal taking a value of 1 ps. Occupation densities decay on a longer time-scale due to recombination processes[67] and we have used a value of 90 ps for this decay rate, i.e., there is practically no recombination on the time scale of our experiment. We also used an inhomogeneous broadening of 1 meV in all calculations. The microscopic modeling of dephasing is an interesting subject in its own right, which continues to attract much attention.[67–72] However, the dephasing of high-order correlations and/or spectrally sharp structures such as the exciton or the biexciton at low-temperatures and low-excitation densities is still not well understood.[25] A microscopic treatment of dephasing is beyond the scope of this paper. Previous calculations of FWM signals[27] have shown that significant fifth-order contributions are obtained for a pulse area of $A = 0.026$. In order to account for the slightly higher excitation densities needed in our present experiment to combat the noise level, we show in the following calculations performed with $A = 0.03$. However, as precise absolute values for A are not easily extracted from the experiment, we have verified that a pulse area of $A = 0.04$ yields very similar results (not shown) leading to the same conclusions.

V. COMPARISON BETWEEN EXPERIMENT AND THEORY

Figure 4(a) shows $S_{SWM}(\Delta t, \omega)$ calculated for the $\{x,y,y\}$ configuration using the full set of equations presented in the previous section. As in the experiment, there are strong emissions at the exciton position, as well as one biexciton binding energy below. Also in agreement with the measurements, a smooth decay is seen as a function of Δt and there is no beating. It has already been pointed out in Ref. 50 that these features can only be reproduced when IDAT contributions
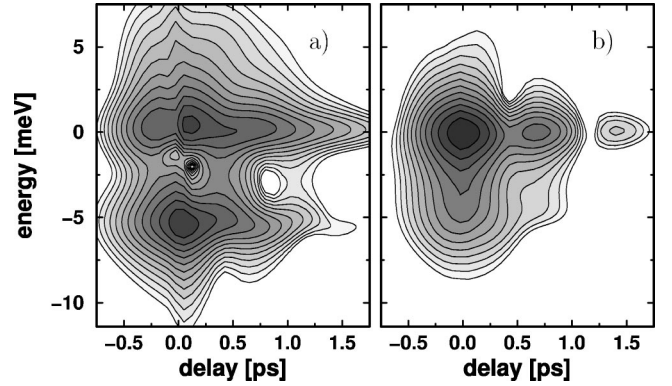
FIG. 4. SWM emission calculated on the IDAT level including two-, four-, and six-point contributions $Y, \bar{B}, \bar{N}$, and $\bar{Z}$: (a) in the $\{x,y,y\}$ configuration, (b) in the $\{x,x,x\}$ configuration. The energy is relative to the exciton transition.

are included. Calculations in the coherent limit yield an almost vanishing EBT emission, which is at least two orders of magnitude too low [see Fig. 2(a) in Ref. 50]. The CL calculation correctly shows no beats in the exciton emission, but this is no surprise, as the EBT contribution is greatly underestimated. This inability of CL calculations to reproduce the relative weights of exciton and biexciton contributions to SWM is in sharp contrast to the FWM results. The inclusion of $\mathcal{Q}_{ID}$, which did reproduce even small details of FWM signals from the same and similar samples,[27,28] actually produces even more significant discrepancies from the SWM experiments [cf. Fig. 2(b) in Ref. 50]. The ID calculation still underestimates the EBT contribution, and shows strong beats at the exciton position.[50] Thus, the six-point correlation $\bar{Z}$ is absolutely necessary to describe accurately the results of the SWM experiments.

It is interesting to study the relative influence of the bound biexciton X_2 and of the two-pair scattering continuum X-X on the IDAT part of the dynamics. This is easily achieved in our calculation by keeping either only the X_2 or only the X-X parts of the memory kernel $\mathcal{K}(t)$ in the expression (6) of $\mathcal{Q}_{IDAT}^{\alpha}$. The results are shown in Fig. 5(a) and 5(b), where in Fig. 5(a) the X_2 contribution has been switched off, while in
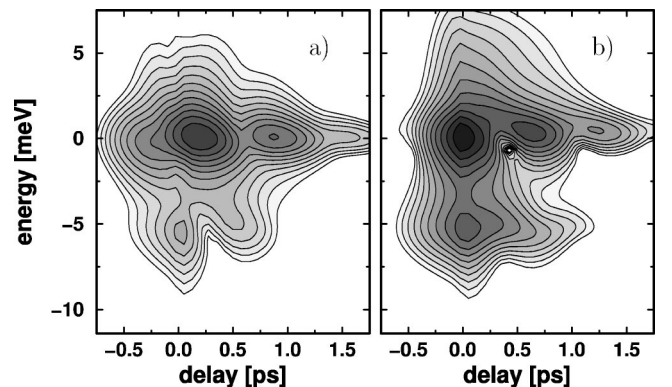
FIG. 5. SWM emission in the $\{x,y,y\}$ configuration: (a) calculation without the IDAT to the biexciton molecule, (b) calculation without the IDAT to the two-pair continuum.
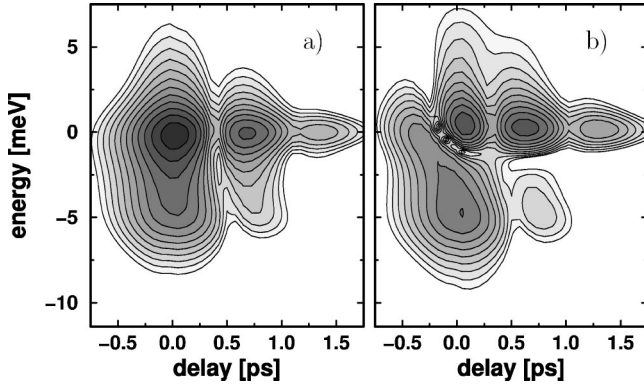
FIG. 6. SWM emission in the $\{x,x,x\}$ configuration: (a) calculation in the coherent limit CL, (b) calculation on the ID level.

Fig. 5(b) it is the X-X contribution that is left out. In Fig. 5(a), the magnitude of the signal at the EBT energy dramatically drops in accordance with the previous finding that the coherent two-pair transitions to the biexciton molecule, which are still included in the calculation, are too weak to explain this emission (cf. the discussion of the coherent limit). The X_2 emission is of course stronger in Fig. 5(b). However, in contrast with the full calculation in Fig. 4(a) and with the experiment, it is still much weaker than the exciton emission. As mentioned earlier, strong cancellations between the continuum of two-pair transitions and the coherent mean-field contributions occur, leading to an overestimate of the exciton contribution in the FWM signals when the two-pair continuum is switched off.[41,62] The results of Fig. 5(b) indicate a similar behavior of the incoherent parts of the dynamics. Neglecting the IDAT continuum also leads to an overestimate of the exciton contribution, thus demonstrating compensations between direct ID parts and the IDAT continuum in the full calculation in Fig. 4(a). Another remarkable aspect of the comparison is that Fig. 5(a), as well as Fig. 5(b), show beats at the exciton energy and additional beats are seen at the EBT energy in Fig. 5(a). Obviously, the incoherent discrete transitions have not only significant influence on the signal at the EBT energy (which is expected) but also strongly modify the signal at the exciton energy. This mixing of discrete and continuum parts of the dynamics is due to the high-order nonlinearities detected in SWM experiments. The suppression of beats at both exciton energy and EBT energy thus requires a subtle balance between the discrete and continuum contributions of $\bar{Z}$.

Figure 4(b) shows the result of a calculations on the full IDAT level for the $\{x,x,x\}$ configuration. We compare this with calculations in the coherent limit in Fig. 6(a), and invoking the ID level in Fig. 6(b). Interestingly, for the $\{x,x,x\}$ configuration all three levels of the theory are able to reproduce a beating at the exciton energy. However, it is found experimentally that there is only a very weak emission at the EBT energy, and this agrees only with the CL and IDAT calculation. In contrast, the ID calculation predicts a much too strong emission at the EBT position. Thus, we find again, a strong competition between the contributions from $\mathcal{Q}_{ID}^{\alpha}$ and $\mathcal{Q}_{IDAT}^{\alpha}$.

Some features of the experimental data are, however, not reproduced even at the IDAT level. For example, in the $\{x,x,x\}$ configuration the beats are significantly slanted on the energy/time-delay axis, an effect that is not evident in any of the theoretical plots. As mentioned above, there are still a number of potential high-order contributions to the SWM signals, whose influence has not yet been explored. These include contributions of correlated three-pair transitions and incoherent two-pair occupations. At present, we are unable to discriminate among these possible explanations, and further work is needed.

As discussed before, the signals for the $\{\sigma^+,\sigma^+,\sigma^+\}$ and the $\{x,\sigma^+,\sigma^+\}$ configurations should be the same at the $\chi^{(5)}$ level. This selection rule can be derived by straightforward algebra using the standard representations of the dipole matrix elements for the heavy-hole transitions. A more intuitive understanding is gained from the following argument: when only fifth-order processes are taken into account there are six waves participating in the buildup of a polarization in direction $\vec{k}_s = 3\vec{k}_2 - 2\vec{k}_1$, three incoming waves in direction $\vec{k}_2$, two out-going waves in direction $\vec{k}_1$, and the out-going signal in direction $\vec{k}_s$. The three incoming $\vec{k}_2$ waves originate from σ^+ photons. Thus, for a σ^+ signal wave, the balance of angular momentum requires that only the σ^+ photons from the x-polarized k_1 waves participate. However, biexciton molecules can only be excited by photons with opposite angular momentum, which is therefore not possible in a $\chi^{(5)}$ process in the $\{x,\sigma^+,\sigma^+\}$ configuration. On the other hand, in seventh order in the laser field, the selection rules allow a broader variety of polarization combinations, and consequently, these signals for $\{\sigma^+,\sigma^+,\sigma^+\}$ and $\{x,\sigma^+,\sigma^+\}$ may differ. In particular, the processes involving two or more waves in $\vec{k}_1$ direction (with change of sign $\vec{k}_1 \rightarrow -\vec{k}_1$ coming from the phase conjugation of some variables) according to $3\vec{k}_2 - 2\vec{k}_1 + n \times (\vec{k}_1 - \vec{k}_1) \rightarrow \vec{k}_s$ are good candidates for an explanation of the observed differences between these configurations. An example of a process of this type that is included in our present treatment can be identified from the analysis of the contribution from two-pair transitions, which is proportional to $\sim Y^* \bar{B}$. In the first step, a biexciton molecule can be formed from photons with opposite circular polarization taken from the $\vec{k}_1$ wave. The resulting second-order $\bar{B}_{2\vec{k}_1}^{(2)}$ in direction $2\vec{k}_1$ gives, together with the first-order polarization $Y_{\vec{k}_1}^{(1)}$, a source for an x polarized third-order polarization $Y_{\vec{k}_1}^{(3)}$ in $\vec{k}_1$ direction $\sim Y_{\vec{k}_1}^{(1)*} \bar{B}_{2\vec{k}_1}^{(2)}$ that contains frequency components at the EBT energy. In a similar way, a third-order polarization $Y_{2\vec{k}_2-\vec{k}_1}^{(3)}$ can be generated in direction $2\vec{k}_2 - \vec{k}_1$. In contrast to the first case, due to the circular polarization of $\vec{k}_2$, this polarization does not involve a biexciton molecule. Combining $Y_{2\vec{k}_2-\vec{k}_1}^{(3)}$ with the linear response $Y_{\vec{k}_2}^{(1)}$, a fourth-order $\bar{B}_{3\vec{k}_2-\vec{k}_1}^{(4)}$ is generated, which provides a source $\sim Y_{\vec{k}_1}^{(3)*} \bar{B}_{3\vec{k}_2-\vec{k}_1}^{(4)}$ for a seventh-order polarization in $3\vec{k}_2 - 2\vec{k}_1$ direction. This term has biexcitonic contributions
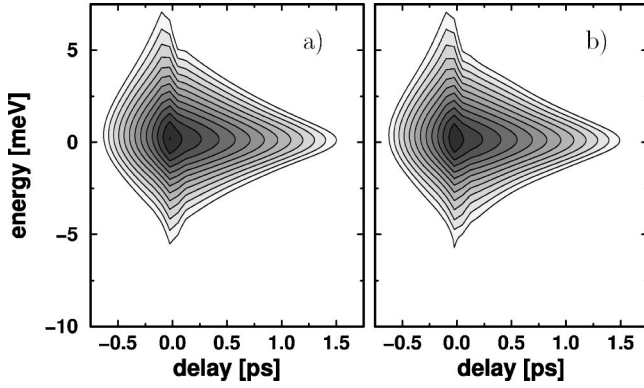
FIG. 7. SWM emission calculated on the IDAT level. (a) in the $\{\sigma^+,\sigma^+,\sigma^+\}$ configuration, (b) in the $\{x,\sigma^+,\sigma^+\}$ configuration.

from $Y_{k_1}^{(3)*}$; which would be impossible in the $\{\sigma^+,\sigma^+,\sigma^+\}$ configuration.

The theoretical results obtained on the IDAT level for excitations involving circular polarized pulses are shown in Fig. 7. The plot for the $\{\sigma^+,\sigma^+,\sigma^+\}$ configuration in Fig. 7(a) is in good agreement with the experiment, which is not surprising, because due to the total absence of biexcitons, this configuration is quite insensitive to the level of theory used. Figure 7(b) shows $\{x,\sigma^+,\sigma^+\}$ data. Obviously, there is no significant difference in the numerical results for $\{\sigma^+,\sigma^+,\sigma^+\}$ and the $\{x,\sigma^+,\sigma^+\}$ configuration seen over the three orders of magnitude displayed in the figure. However, for the $\{x,\sigma^+,\sigma^+\}$ configuration, the calculation yields a weak $\chi^{(7)}$ signal at the EBT energy that is far off scale in Fig. 7 and much weaker than in the experiment. Although many of the $\chi^{(7)}$ processes that do involve the biexciton molecule in the $\{x,\sigma^+,\sigma^+\}$ case are included in our calculation (see above), there is no indication for the experimentally observed modulation. This result remains unchanged even when higher excitation densities are used (we tested $A=0.05$ and $A=0.1$), where strong saturation effects due to Pauli blocking become relevant (not shown). We therefore conclude that the observed modulation in the $\{x,\sigma^+,\sigma^+\}$ configuration is not only a clear indication for $\chi^{(7)}$ contributions, it must also be attributed to processes that go beyond the high-order correlations taken into account in the present calculations.

VI. CONCLUSION

Investigations of high-order correlations using the SWM technique have only just begun; but already on the basis of the experimental and theoretical data presented in this paper several conclusions can be drawn. The comparison between measurements and calculations at different levels of approximation clearly reveals that six-point correlations are indispensable for a microscopic understanding of SWM. In contrast to FWM, we find a much higher sensitivity of SWM signals to correlations beyond the four-point level. In fact, we have demonstrated that it is possible to excite a semiconductor in such a way that strong correlations among six or more particles are induced, which is not evident from FWM.

However, some of the observations turn out to be even beyond the present treatment, where six-point correlations representing incoherent density assisted transitions have been included. Examples are the slanting of the beats seen in the $\{x,x,x\}$ configuration or the modulation of the $\{x,\sigma^+,\sigma^+\}$ signal. The latter has been shown to be due to at least a $\chi^{(7)}$ process.

Using linearly polarized pulses for the excitation, we have found a remarkable dynamical decoupling between spectral features and beating in the time-delay regime. While in the $\{x,y,y\}$ configuration a strong spectral contribution of the biexciton is not associated with beats in the time delay, strong beating is observed in the $\{x,x,x\}$ case, although there is only a very weak emission at the EBT energy. We have shown that this dynamical decoupling is well reproduced by the DCT theory, but only when IDAT contributions are included. Finally, an analysis of the IDAT contributions of the biexciton molecule and the two-pair continuum reveals partial compensation effects between the ID and the IDAT continuum, as well as a strong mixing between the discrete and continuous IDAT components.

APPENDIX: TREATMENT OF INCOHERENT CONTRIBUTIONS TO THE DYNAMICS

In this appendix we outline the treatment of the incoherent densities $\bar{N}$ used in this paper and derive the memory kernel representation for the IDAT contributions. Our starting point is the equation of motion for the pair density N [Eq. (39) of Ref. 10], which has been derived by applying the DCT scheme at the third order. Switching to the exciton representation, this equation reads

$$\hbar[-i\partial_t+\omega_\alpha-\omega_\alpha^-]n_{\bar{\alpha}\alpha}=\sum_p \mathcal{M}_\alpha^p E_{\text{opt}}^p y_\alpha^* - \sum_p \mathcal{M}_\alpha^{p*} E_{\text{opt}}^{p*} y_\alpha.$$

(A1)

Using Eq. (A1) together with Eq. (1), we immediately obtain the desired equation for the incoherent part $\bar{n}_{\bar{\alpha},\alpha}=n_{\bar{\alpha}\alpha}-y_\alpha^* y_\alpha$ of the pair density

$$\hbar[-i\partial_t+\omega_\alpha-\omega_\alpha^-]\bar{n}_{\bar{\alpha}\alpha}=\mathcal{Q}_{\text{nonlinear}}^{\bar{\alpha}*}y_\alpha - y_\alpha^*\mathcal{Q}_{\text{nonlinear}}^\alpha,$$

(A2)

where $\mathcal{Q}_{\text{nonlinear}}^\alpha$ is the nonlinear source of the y equation. The $\bar{n}$ equation would contain further sources if, in addition, phonons or other bath couplings had been taken into account.[40] However, phonons are expected to be of minor

importance at the low temperatures considered here, which is confirmed by the good agreement with FWM experiments[27,28] obtained by using Eq. (A2).

In order to derive the memory kernel representation for the IDAT contributions, we start from the equation of motion for $\bar{Z}$ given in Ref. 40 in the Wannier representation. As in the $\bar{N}$ case, we neglect the phonon-induced parts derived in Ref. 40 leading to

$$\hbar[-i\partial_t + \Omega_{B_{46}^{35}} - \Omega_{Y_1^2}]\bar{Z}_{146}^{235} = V(^3_4|^5_6)(\bar{N}_{14}^{23}Y_6^5 + \bar{N}_{16}^{25}Y_4^3)$$
$$- V(^3_6|^5_4)(\bar{N}_{16}^{23}Y_4^5 + \bar{N}_{14}^{25}Y_6^3),$$

(A3)

where $\hbar\Omega_Y$ and $\hbar\Omega_B$ are the Hamiltonians for the single and the two-pair problem, respectively (cf. Ref. 10) and with $V(^1_2|^3_4) \equiv V_{14} + V_{23} - V_{13} - V_{24}$, where V_{12} is the Coulomb potential. Thus, the eigenenergies of the oscillators represented by $\bar{Z}$ are differences between one- and two-pair energies as expected for transitions from single-pair to two-pair states. The sources on the right-hand side of Eq. (A3) are proportional to $Y\bar{N}$, confirming the interpretation as incoherent density-assisted transitions. In particular, in the absence of incoherent densities $\bar{N}$, those transitions are not generated. In an analogy to the treatment of the two-pair transitions,[41] we formally invert Eq. (A3) by using the corresponding Green function G_Z. Noting that $\hbar\Omega_Y$ and $\hbar\Omega_B$ act on different sets of variables, we find that G_Z is given by a product of the complex conjugate of the Green function G_Y for the single-pair problem and the two-pair Green function G_B defined in Ref. 41. We thus obtain the following formal solution of equations (A3)

$$\bar{Z}_{146}^{235}(t) = \int_{-\infty}^t dt' \sum_{\substack{2'3'5'\\1'4'6'}} i\hbar G_Y^*(^2_1,^{2'}_{1'};t-t')G_B(^{35}_{46},^{3'5'}_{4'6'};t-t')$$

$$\times \{V(^{3'}_{4'}|^{5'}_{6'})[\bar{N}_{1'4'}^{2'3'}(t')Y_{6'}^{5'}(t') + \bar{N}_{1'6'}^{2'5'}(t')Y_{4'}^{3'}(t')]$$

$$- V(^{3'}_{6'}|^{5'}_{4'})[\bar{N}_{1'6'}^{2'3'}(t')Y_{4'}^{5'}(t') + \bar{N}_{1'4'}^{2'5'}(t')Y_{6'}^{3'}(t')]\}.$$

(A4)

It is tempting to think that the factorization property of the $\bar{Z}$-Green function would mean that only correlations between

the particles at sites {1,2} and among those at {3,4,5,6} are built up, so that $\bar{Z}$ would not contain correlations where six particles participate. However, looking at the sources for $\bar{Z}$, a different picture is obtained. Here, the particles at {1,2} are always correlated to another electron-hole pair selected from the particles at {3,4,5,6} by means of a four-point correlation $\bar{N}$. In fact, all possible combinations for the above selection do show up. If we follow the fate of a particular contribution to $\bar{Z}$, e.g., the one arising from the source $\sim\bar{N}_{14}^{23}Y_6^5$, we see that a genuine six-particle correlation is indeed builtup sequentially; in a first step, the Coulomb interaction leads to a correlation $\bar{N}_{14}^{23}$ between the pair at {1,2} and another pair at {3,4}, while a third pair at {5,6} is uncorrelated after this step. Then, the source $\sim\bar{N}_{14}^{23}Y_6^5$ is propagated by means of the $\bar{Z}$ Green function, which introduces a new correlation between the pairs {3,4} and {5,6} [see Eq. (A4)]. The result of this two-step process is a correlation involving six-particles, although there is no direct Coulomb interaction in the $\bar{Z}$ propagator between the particle at {1,2} and those at {3,4,5,6}, which would be the case for the correlated three-pair transition density.[73]

The contribution of $\bar{Z}$ to the equation of motion for y_α is according to Refs. 40 and 11 given by

$$\mathcal{Q}_{\text{IDAT}}^\alpha = \sum_{12lj} \frac{1}{\sqrt{\Omega}} \phi_\alpha^*(^1_2)V(^1_2|^l_j)\bar{Z}_{jj2}^{l l 1},$$

(A5)

where $\phi_\alpha(^1_2)$ is the wave function of exciton α and Ω is a normalization volume. We now insert Eq. (A4) on the right-hand side of Eq. (A5) and invoke the exciton representations for Y and $\bar{N}$. The lengthy expression obtained in this way can be simplified by using the standard expansion of G_Y in terms of exciton wave functions

$$G_Y(^2_1,^{2'}_{1'};t) = \frac{i}{\hbar} \sum_\alpha \phi_\alpha(^2_1)\phi_\alpha^*(^{2'}_{1'})\theta(t)e^{-i\omega_\alpha t},$$

(A6)

because with the help of Eq. (A6) the sums over 1′ and 2′ in Eq. (A4) can be performed, taking into account the orthonormalization of the exciton wave functions. Collecting the remaining eightfold space summations we recover the definition of the memory kernel $\mathcal{K}$ for the two-pair transitions [Eq. (5) in Ref. 41] and thus finally arrive at the representation (6) for the IDAT sources $\mathcal{Q}_{\text{IDAT}}^\alpha$.

---

*Permanent address: Physics Department, Williams College, Williamstown, MA 01267.

†Permanent address: Institut für Festkörperphysik, Universität Bremen, P.O. Box 330 440, D-28334 Bremen, Germany.

‡Permanent address: Department of Physics, University of California at San Diego, La Jolla, CA 92093-0319.

[1] E. Hagley, X. Matre, G. Nogues, C. Wunderlich, M. Brune, J. M. Raimond, and S. Haroche, Phys. Rev. Lett. **79**, 1 (1997).

[2] H. Haug and A. P. Jauho, *Quantum Kinetics for Transport and Optics in Semiconductors*, Solid-State Sciences Vol. 123 (Springer, Berlin, 1996).

[3] T. Kuhn, in *Theory of Transport Properties of Semiconductor Nanostructures*, edited by E. Schöll (Chapman and Hall, London, 1998), p. 173.

[4] M. Bonitz, *Quantum Kinetic Theory*, Teubner-Texte zur Physik Vol. 33 (Teubner-Verlag Stuttgart/Leipzig, 1998).

[5] M. Bonitz, J. W. Dufty, and C. S. Kim, Phys. Status Solidi B **206**, 181 (1998).

[6] U. Hohenester and W. Pötz, Phys. Rev. B **56**, 13 177 (1997).

[7] U. Hohenester, F. Rossi, and E. Molinari, Solid State Commun. **111**, 187 (1999).

[8] M. F. Pereira and K. Henneberger, Phys. Rev. B **58**, 2064 (1998).

[9] A. L. Ivanov, H. Haug, and L. V. Keldysh, Phys. Rep. **296**, 237 (1998).

[10] V. M. Axt and A. Stahl, Z. Phys. B: Condens. Matter **93**, 195 (1994); **93**, 205 (1994).

[11] V. M. Axt and S. Mukamel, Rev. Mod. Phys. **70**, 145 (1998).

[12] M. Bonitz, D. Semkat, and H. Haug, Eur. Phys. J. B **9**, 309 (1999).

[13] M. Z. Maialle and L. J. Sham, Phys. Rev. Lett. **73**, 3310 (1994).

[14] N. H. Kwong and R. Binder, Phys. Rev. B **61**, 8341 (2000).

[15] M. F. Pereira and K. Henneberger, Phys. Status Solidi B **206**, 477 (1998).

[16] W. Schäfer, R. Lövenich, N. Fromer, and D. S. Chemla, Phys. Status Solidi B **221**, 195 (2000).

[17] D. S. Chemla, J.-Y. Bigot, M.-A. Mycek, S. Weiss, and W. Schäfer, Phys. Rev. B **50**, 8439 (1994).

[18] D. S. Chemla and J. Y. Bigot, Chem. Phys. **210**, 135 (1995).

[19] S. Bar-Ad, P. Kner, M. V. Marquezini, K. El Sayed, and D. S. Chemla, Phys. Rev. Lett. **77**, 3177 (1996).

[20] F. X. Camescasse, A. Alexandrou, D. Hulin, L. Bányai, D. B. Tran Thoai, and H. Haug, Phys. Rev. Lett. **77**, 5429 (1996).

[21] Q. T. Vu, L. Bányai, P. I. Tamborenea, and H. Haug, Europhys. Lett. **40**, 323 (1997).

[22] Q. T. Vu, L. Bányai, H. Haug, F. X. Camescasse, J. P. Likforman, and A. Alexandrou, Phys. Rev. B **59**, 2760 (1999).

[23] L. Bányai, Q. T. Vu, B. Mieck, and H. Haug, Phys. Rev. Lett. **81**, 882 (1998).

[24] P. Kner, S. Bar-Ad, M. V. Marquezini, D. S. Chemla, and W. Schäfer, Phys. Rev. Lett. **78**, 1319 (1997).

[25] P. Kner, W. Schäfer, R. Lövenich, and D. S. Chemla, Phys. Rev. Lett. **81**, 5386 (1998).

[26] P. Kner, S. Bar-Ad, M. V. Marquezini, D. S. Chemla, R. Lövenich, and W. Schäfer, Phys. Rev. B **60**, 4731 (1999).

[27] G. Bartels, A. Stahl, V. M. Axt, B. Haase, U. Neukirch, and J. Gutowski, Phys. Rev. Lett. **81**, 5880 (1998).

[28] B. Haase, U. Neukirch, J. Gutowski, G. Bartels, A. Stahl, V. M. Axt, J. Nürnberger, and W. Faschinger, Phys. Rev. B **59**, R7805 (1999).

[29] T. Östreich, K. Schönhammer, and L. J. Sham, Phys. Rev. B **58**, 12 920 (1998).

[30] W. A. Hügel, M. F. Heinrich, M. Wegener, Q. T. Vu, L. Bányai, and H. Haug, Phys. Rev. Lett. **83**, 3313 (1999).

[31] L. Bányai, D. B. Tran Thoai, E. Reitsamer, H. Haug, D. Steinbach, M. U. Wehner, M. Wegener, T. Marschner, and W. Stolz, Phys. Rev. Lett. **75**, 2188 (1995).

[32] D. Steinbach, M. U. Wehner, M. Wegener, L. Bányai, E. Reitsamer, and H. Haug, Chem. Phys. **210**, 49 (1996).

[33] A. Leitenstorfer, C. Furst, AA. Laubereau, W. Kaiser, G. Trankle, and G. Weimann, Phys. Rev. Lett. **76**, 1545 (1996).

[34] C. Fürst, A. Leitenstorfer, A. Laubereau, and R. Zimmermann, Phys. Rev. Lett. **78**, 3733 (1997).

[35] R. Zimmermann, J. Wauer, A. Leitenstorfer, and C. Fürst, J. Lumin. **76**, 34 (1998).

[36] M. U. Wehner, M. U. Ulm, D. S. Chemla, and M. Wegener, Phys. Rev. Lett. **80**, 1992 (1998).

[37] M. U. Wehner, D. S. Chemla, and M. Wegener, Phys. Rev. B **58**, 3590 (1998).

[38] D. Steinbach, G. Kocherscheidt, and M. U. Wehner, H. Kalt, M. Wegener, K. Ohkawa, D. Hommel, and V. M. Axt, Phys. Rev. B **60**, 12 079 (1999).

[39] U. Woggon, F. Gindele, W. Langbein, and J. M. Hvam, Phys. Rev. B **61**, 1935 (2000).

[40] V. M. Axt, K. Victor, and A. Stahl, Phys. Rev. B **53**, 7244 (1996).

[41] V. M. Axt, K. Victor, and T. Kuhn, Phys. Status Solidi B **206**, 189 (1998).

[42] T. Östreich and L. J. Sham, Phys. Rev. Lett. **83**, 3510 (1999).

[43] A. Stahl, and I. Balslev, *Electrodynamics at the Semiconductor Band Edge*, Springer Tracts in Modern Physics Vol. 110 (Springer, Berlin, 1987).

[44] H. Haug and S. W. Koch, *Quantum Theory of Optical and Electronic Properties of Semiconductors*, 2nd ed. (World Scientific, Singapore, 1993).

[45] T. Meier and S. W. Koch, Phys. Rev. B **59**, 13 202 (1999).

[46] V. M. Axt, B. Haase, J. Meinertz, and U. Neukirch (unpublished).

[47] U. Neukirch, S. R. Bolton, N. A. Fromer, L. J. Sham, and D. S. Chemla, Phys. Rev. Lett. **84**, 2215 (2000).

[48] U. Neukirch, S. R. Bolton, L. J. Sham, and D. S. Chemla, Phys. Rev. B **61**, R7835 (2000).

[49] D. S. Chemla and A. Maruani, Prog. Quantum Electron. **8**, 1 (1982), and references therein.

[50] S. R. Bolton, U. Neukirch, L. J. Sham, D. S. Chemla, and V. M. Axt, Phys. Rev. Lett. **85**, 2002 (2000).

[51] L. J. Sham, Phys. Rev. **150**, 720 (1966).

[52] U. Siegner, M.-A. Mycek, S. Glutsch, and D. S. Chemla, Phys. Rev. Lett. **74**, 470 (1995).

[53] U. Siegner, M.-A. Mycek, S. Glutsch, and D. S. Chemla, Phys. Rev. B **51**, 4953 (1995).

[54] M. U. Wehner, D. Steinbach, and M. Wegener, Phys. Rev. B **54**, R5211 (1996).

[55] D. S. Chemla, A. Maruani, and F. Bonnouvrier, Phys. Rev. A **26**, 3026 (1982).

[56] F. Rossi, S. Haas, and T. Kuhn, Phys. Rev. Lett. **72**, 152 (1994).

[57] S. Haas, F. Rossi, and T. Kuhn, Phys. Rev. B **53**, 12 855 (1996).

[58] G. Manzke, Q. Y. Peng, K. Henneberger, U. Neukirch, K. Hauke, K. Wundke, J. Gutowski, and D. Hommel, Phys. Rev. Lett. **80**, 4943 (1998).

[59] C. Sieh, T. Meier, F. Jahnke, A. Knorr, S. W. Koch, P. Brick, M. Hübner, C. Ell, J. Prineas, G. Khitrova, and H. M. Gibbs, Phys. Rev. Lett. **82**, 3112 (1999).

[60] B. Dick and R. M. Hochstrasser, Chem. Phys. **75**, 133 (1983).

[61] I. Abram, A. Maruani, and S. Schmitt-Rink, J. Phys. C **17**, 5163 (1984).

[62] B. Haase, U. Neukirch, J. Gutowski, J. Nürnberger, W. Faschinger, M. Behringer, D. Hommel, V. M. Axt, G. Bartels, and A. Stahl, J. Cryst. Growth **214**, 856 (2000).

[63] B. Haase, U. Neukirch, J. Gutowski, G. Bartels, A. Stahl, J. Nürnberger, and W. Faschinger, Phys. Status Solidi B **206**, 363 (1998).

[64] M. Lindberg, R. Binder, and S. W. Koch, Phys. Rev. A **45**, 1865 (1992).

[65] T. Kuhn, E. Binder, F. Rossi, A. Lohner, K. Rick, P. Leisching, A. Leitenstorfer, T. Elsaesser, and W. Stolz, in *Coherent Optical Interactions in Semiconductors*, Vol. 330 of *NATO Advanced Studies Institute, Series B: Physics,* edited by R. T. Phillips (Plenum, New York, 1994), p. 33.

[66] W. Langbein and J. M. Hvam, Phys. Rev. B **61**, 1692 (2000).

[67] D. S. Citrin, Phys. Rev. B **47**, 3832 (1993).

[68] O. M. Schmitt, L. Bányai, and H. Haug, Phys. Rev. B **60**, 16 506 (1999).

[69] G. Manzke, U. Moldzio, and K. Henneberger, Phys. Status Solidi B **202**, 961 (1997).

[70] B. Mieck and H. Haug, Phys. Status Solidi B **213**, 397 (1999).

[71] L. Bányai, Q. T. Vu, and H. Haug, Phys. Rev. B **58**, R13 341 (1998).

[72] K. Elsayed, L. Bányai, H. Haug, Phys. Rev. B **50**, 1541 (1994).

[73] K. Victor, V. M. Axt, and A. Stahl, Phys. Rev. B **51**, 14 164 (1995).